Journal of Applied Polymer Science

Real-Time Monitoring of Ring-Opening Polymerization of Tetrahydrofuran via *In Situ* Fourier Transform Infrared Spectroscopy

Hangjun Deng,[1] Zhongquan Shen,[2] Lifeng Li,[2] Hong Yin,[2] Jizhong Chen[1,2]

[1]State Key Laboratory of Chemical Engineering, Department of Chemical and Biological Engineering, Zhejiang University, Hangzhou 310027, China

[2]Research Center of Chemical Reaction Engineering, Department of Chemical and Biological Engineering, Zhejiang University, Hangzhou 310027, China

Correspondence to: H. Yin (E-mail: yinh@zju.edu.cn) and J. Chen (E-mail: chenjz@zju.edu.cn)

ABSTRACT: The polymerization of tetrahydrofuran (THF) was carried out in CH_2Cl_2 by using phosphotungstic heteropolyacid as initiator and epichlorohydrin as promoter. This cationic ring-opening polymerization process was monitored by *in situ* mid-infrared spectroscopy system (ReactIR) to further study the thermodynamics and kinetics of THF polymerization. It was observed that the sharp infrared peak of C—O—C stretching vibrations will shift from about 1068 to 1109 cm^{-1} in THF ring-opening step. The changes in absorbance intensity of the two characteristic peaks were used for determining instantaneous concentration of linear polymer and ring monomer. The experimental results demonstrated that the kinetics of THF polymerization proved to be typically first-order. Thermodynamic parameters were determined from the temperature dependence of the monomer equilibrium concentration $[M]_e$ over the range from −5 to 25°C. The values of k_{app} were obtained via the plots of $\ln\{([M]_0-[M]_e)/([M]_t-[M]_e)\}$ vs reaction time, for polymerization under specific conditions. The apparent activation energy (E_a) and frequency (A) were determined from the Arrhenius plot of k_{app} vs. T^{-1}. Besides, the *in situ* kinetic investigation revealed that more chain-transfer occurred at higher temperatures, leading to a reduction in propagation species concentration and a deviation from first-order propagation at the later stage of polymerization. © 2014 Wiley Periodicals, Inc. J. Appl. Polym. Sci. **2014**, *131*, 40503.

KEYWORDS: *in situ* FTIR; kinetics; phosphotungstic heteropolyacid; ring-opening polymerization; tetrahydrofuran

Received 29 August 2013; accepted 24 January 2014

DOI: 10.1002/app.40503

INTRODUCTION

The polytetrahydrofuran (PTHF) is widely used in thermoplastic elastomers polyurethanes,[1] novel copolymers,[2–5] and composite materials,[5] and is produced through a polymerization reaction of tetrahydrofuran (THF), which is one of the most common cationic ring-opening polymerizations (CROP).[6] It has been demonstrated earlier that CROP of THF proceeds as a process with fast initiation, rapid propagation, uncontrollable chain transfer, and non-termination,[7] which is closely connected to the yield and molecular weight of PTHF product. Hence, the kinetic understanding of THF polymerization reaction is of great importance not only from fundamental science but also from industrial points of view.

In cationic polymerization, it is generally reported that both the free oxonium ion and ion-pair generated in initiation step contribute to propagations.[8] Since the first report on CROP of THF,[9] numerous efforts have been devoted to the studies of the initiation and the first-order reversible propagation.[10–17] In recent years, heteropolyacid such as phosphotungstic acid (HPW) has been proved to be an efficient and promising initiator for THF polymerization promoted by heterocycles,[18–21] and their kinetic investigation of HPW initiating polymerization was based on the assumption that the active species concentration is triple the concentration of HPW. However, it is worth noting that not all of protons in HPW could be effective during polymerization due to the equilibrium of initiation reactions or to the reduction of propagation species in the unavoidable chain transfer reaction.[22] The phenomenon would be more obvious at higher reaction temperatures.

In the past few years, a number of papers are concerned in the kinetic investigations by using off-line analysis techniques, such as gravimetric method,[23] ^{1}H nuclear magnetic resonance (^{1}H NMR),[10,17] gas chromatography,[6,20,21] UV–visible spectrophotometric technique,[16] and dilatometer.[14,24] However, these studies mostly focused on the early stage of polymerization with low

Additional Supporting Information may be found in the online version of this article.

conversion due to the limitation on the aforementioned techniques. With regard to the THF polymerization, the increasing viscosity of reaction mixture as polymerization proceeds will lead to great difficulty in sampling from the highly viscous reaction mixture.[17] Meanwhile, the volume of reaction mixture decreases as polymerization proceeds, which gives rise to errors in determining the instantaneous concentration of monomer through sampling for off-line analysis. Besides, it is really difficult to judge whether the thermodynamic equilibrium of THF polymerization reaches or not by using off-line analysis techniques. Therefore, the application of real-time analysis system is of great significance in increasing accuracy, reducing laborious sampling, and fully understanding the thermodynamics and kinetics of THF polymerization.

Over the last few years, an *in situ* Fourier Transform Infrared Spectroscopy (FTIR) technique ReactIR™ has been increasingly applied to different polymerization reactions.[25–28] This powerful technique used in conjunction with a remote silicon-attenuated total reflectance (ATR) probe enables the real-time monitoring of reactions without laborious and time-consuming sampling of aliquots.

In this work, ReactIR-based *in situ* monitoring was applied to track the CROP of THF initiated by epichlorohydrin (ECH)/HPW in CH_2Cl_2. The absorbance variation of characteristic peaks versus reaction time was real-timely observed and easily recorded by *in situ* FTIR during the whole process of THF polymerization. The effects of reaction temperature and initiator concentration on kinetics of THF polymerization were systematically investigated. In addition, samples of reaction mixture at different reaction times were also collected for ^{1}H NMR analysis to compare with the results determined by ReactIR.

EXPERIMENTAL

Materials

THF (AR grade, ≥99%) was dried by refluxing over sodium/diphenylketone in nitrogen atmosphere until a blue color appeared and then distilled out. Dichloromethane (AR grade, ≥99.5%) and ECH (AR grade, ≥99%) were dried with calcium hydride in nitrogen atmosphere and distilled off prior to use. HPW (AR) purchased from Sinopharm Chemical Reagent was dried at 170°C for 2 h. PTHF ($M_n \approx 2000$) used as standard polymer with the following structure was purchased from Shanghai Aladdin®, China.

$$HO\text{—}\left(CH_2CH_2CH_2CH_2\text{—}O\right)_n H$$

Polymerization Procedure and Data Acquisition

All *in situ* FTIR polymerizations were performed using a spectrum of nitrogen as reference background and carried out in a stirred nitrogen-purged 100 mL flask. In a typical polymerization, 0.4 g dried HPW was added into the flask. The ReactIR IC10 was equipped with a silicon ATR probe which was directly inserted into the flask. After the flask was nitrogen-purged on a desired temperature, the background spectrum was collected. Then, the flask was charged with 20 mL purified dichloromethane, 20 mL purified THF, and 3 mL ECH by injection. At the same time, the ReactIR monitoring system started to record the spectra continuously every 30 s. After a predetermined time, the reaction was terminated by the addition of 10 mL water and the spectra of the polymerization had been recorded. The reaction mixture was transferred to a separatory funnel followed by aqueous extraction. The organic phase was concentrated on a rotary evaporator. Then, the product was dried at 333 K under vacuum for 6 h.

Characterization

^{1}H NMR analysis for comparing with *in situ* FTIR system was conducted on a Bruker Avance DMX 400 MHz spectrometer using $CDCl_3$ as solvent. Samples of reaction mixture were taken at various reaction time intervals during the polymerization, terminated with a trace of water, and analyzed by ^{1}H NMR. As shown in Figure S1 (Supporting Information), the ^{1}H NMR (400 MHz $CDCl_3$, δ) at 1.8 and 1.6 ppm were used to determine the conversion of monomer THF.

Number-average molecular weight (M_n), weight-average molecular weight (M_w), and PDI (M_w/M_n) of PTHF were measured by gel permeation chromatography (Waters 1525 binary HPLC pump, Waters refractive index detector, Waters 717 autosampler). The samples were dried under vacuum at 60°C for 2 h and then dissolved in THF. The eluent was THF at a flow rate of 1.0 mL min^{-1}, and the measure temperature was 30°C. The molecular weights and PDI were derived from a calibration curve using narrow polystyrene as standard.

RESULTS AND DISCUSSION

In Situ FTIR Data and Analysis

Figure 1 shows the infrared spectra of pure ECH, THF, and CH_2Cl_2 collected by ReactIR. It can be clearly found from Figure 1 that there are two dominant peaks at 911 and 1068 cm^{-1} in the infrared spectrum of THF, which is different from ECH and CH_2Cl_2. But there will be some overlapping bands at 911 cm^{-1} in the reaction mixture, and the absorbance at 911 cm^{-1} is remarkably weaker than that at 1068 cm^{-1}. Thus, the peak at 1068 cm^{-1} ascribed to the antisymmetric stretching vibration frequency of C—O—C is much more suitable to be used for characterizing THF than the peak at 911 cm^{-1}. In the case of heterocyclic polymerization, the antisymmetric stretching vibration frequency of C—O—C in heterocyclic monomer is located at 1070 cm^{-1}, while that in saturated aliphatic ether is located at 1110 ~ 1125 cm^{-1}.[29] Thus, the interesting feature of THF ring-opening step is that the sharp infrared peak of C—O—C will shift from about 1070 cm^{-1} to 1110 ~ 1125 cm^{-1}, allowing a rapid *in situ* tracking of the ring monomer and linear polymer in the polymerization process. As shown in Figure 2, the infrared absorbance at 1109 cm^{-1} increased and that at 1068 cm^{-1} decreased with progressing reaction, implying that the ring-opening polymerization of THF was successfully observed by ReactIR technique. It was pointed out that the absorbance intensity of the characteristic peaks is closely related to the concentrations of the monomer and polymer.[26] Therefore, the two characteristic peaks at 1109 and 1068 cm^{-1} were employed for determining instantaneous concentration of the polymer and monomer, respectively. Prior to kinetic investigations, a number of calibrations of THF and PTHF were conducted to determine the functional relationship between the concentration and characteristic peak intensity. For more details

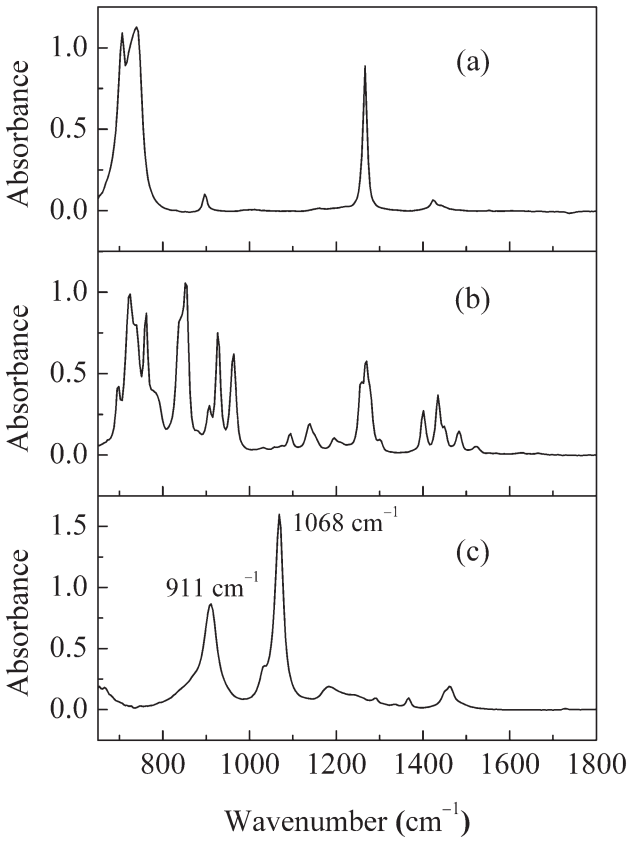

Figure 1. Infrared spectra of (a) CH_2Cl_2, (b) ECH, and (c) THF.

on the calibrations see the Supporting Information (Figure S2). Moreover, we made a reasonable simplification for the calibration curves according to Table S1 (Supporting Information) that the effect of temperature on the infrared absorbance of characteristic peaks could be neglected over the range from −5 to 25°C.[30]

Furthermore, the usefulness of ReactIR as a powerful tool to track the kinetics of the ring-opening polymerization of THF

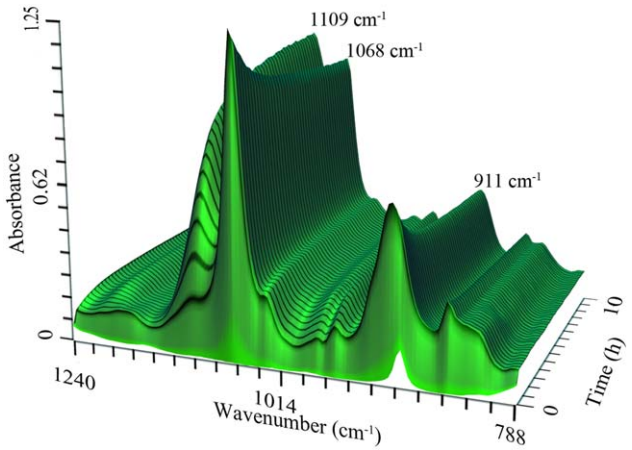

Figure 2. Time dependent IR spectra monitored by ReactIR for THF polymerization at 15°C. Reaction conditions: CH_2Cl_2, 8 mL; THF, 20 mL; HPW, 0.3 g; ECH, 3 mL. [Color figure can be viewed in the online issue, which is available at wileyonlinelibrary.com.]

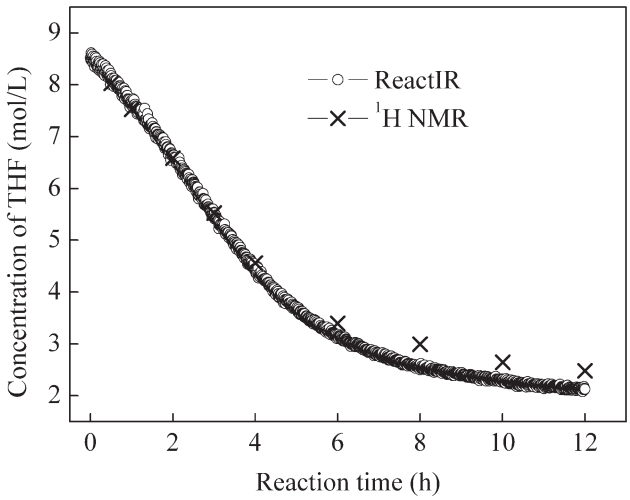

Figure 3. Comparison of the concentration of THF versus time curves determined by both (○) the ReactIR technique and (×) the ^{1}H NMR analysis for the ring-opening polymerization of THF. Reaction conditions: 5°C, 20 mL THF, 3 mL ECH, 0.3 g HPW, 8 mL CH_2Cl_2.

was verified by comparing with ^{1}H NMR method (see Figure S1 in Supporting Information). As can be seen in Figure 3, the concentration of THF measured by ^{1}H NMR is slightly higher than that determined by ReactIR at the later stage of polymerization. An explanation is the increasing viscosity of reaction mixtures at the later stage of polymerization,[17] leading to PTHF polymer stick on the wall of sampler during sampling.

Reaction Mechanism Analysis

Due to the low reactivity of THF, the oxirane with high ring strain, acting as promoter, can considerably speed up the rate of initiation in THF polymerization.[21] Kinetic analysis is based on the reaction pathway proposed to be three reaction steps by Bednarek.[22] However, in cationic polymerization of THF, the propagation active species consist of free oxonium ion and ion-pair.[31] Based on these, we proposed a plausible mechanism of THF polymerization using ECH as promoter (see Scheme 1).

Thermodynamic Investigations

In a first series of experiments, the ring-opening polymerization of THF has been initiated by HPW in CH_2Cl_2 for a constant

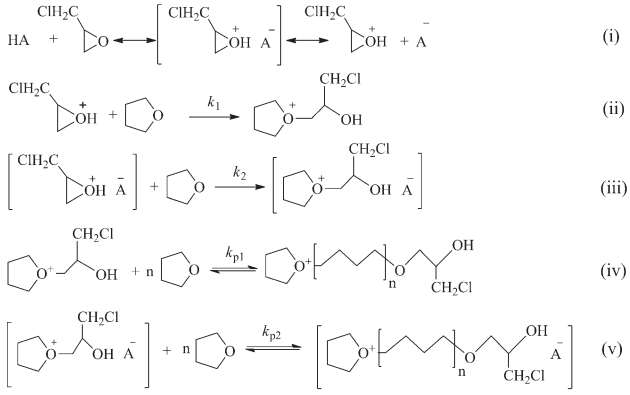

Scheme 1. Plausible mechanism of THF polymerization using epichlorohydrin as promoter

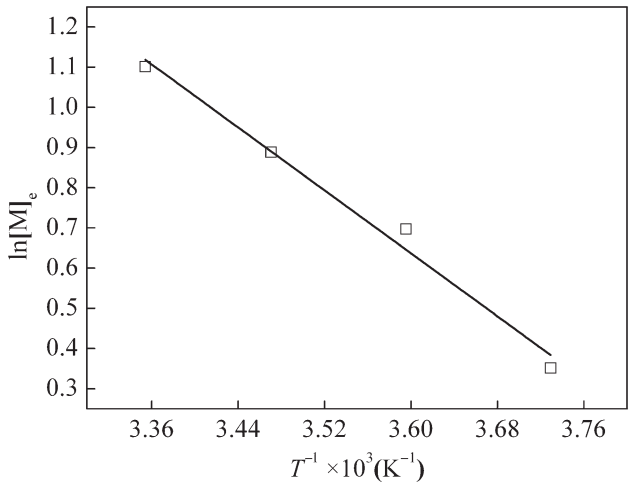

Figure 4. Plot of $\ln[M]_e$ versus T^{-1} with the linear equation: $\ln[M]_e = -1958.75 \times T^{-1} + 7.688$, $R^2 = 0.981$.

monomer-to-promoter molar ratio ($[THF]_0/[ECH]$) of 6.4 at temperature ranging from −5 to 25°C. Figure S3 shows the time dependence of THF concentration determined from *in situ* FTIR results at various temperatures. THF concentration decreases with increasing reaction time until the thermodynamic equilibrium of THF polymerization reaches after a period of reaction time long enough. As shown in Figure S3, the thermodynamic equilibrium at −5, 5, 15, and 25°C were achieved for 30, 14, 10, and 6 h, respectively. Subsequently, the equilibrium concentrations $[M]_e$ of monomer at different reaction temperatures could be obtained from Supporting Information Figure S3.

It is well accepted that the monomer-polymer equilibrium can adequately be described by microreversibility mechanism[32] as eq (1). According to this, the thermodynamic equilibrium constant K for THF polymerization can be given as $1/[M]_e$.

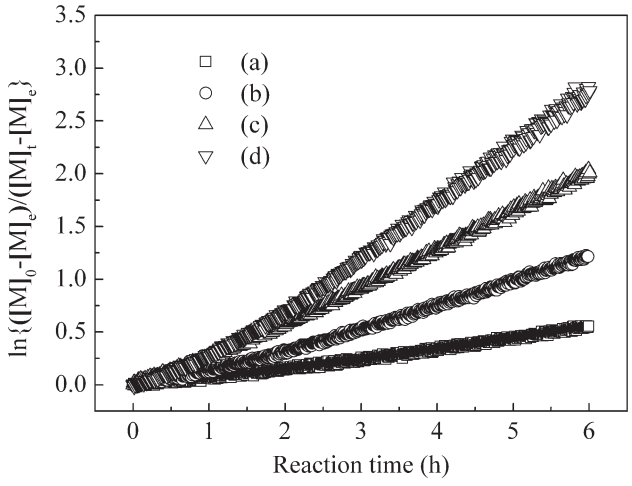

Figure 5. Effect of initiator concentration on the rate of THF polymerization at 5°C. (a) [HPW] = 1.2×10^{-3} mol L^{-1}, (b) [HPW] = 2.4×10^{-3} mol L^{-1}, (c) [HPW] = 3.6×10^{-3} mol L^{-1}, and (d) [HPW] = 4.8×10^{-3} mol L^{-1}. Reaction conditions: THF, 20 mL; CH_2Cl_2, 8 mL; ECH, 3 mL, 6 h.

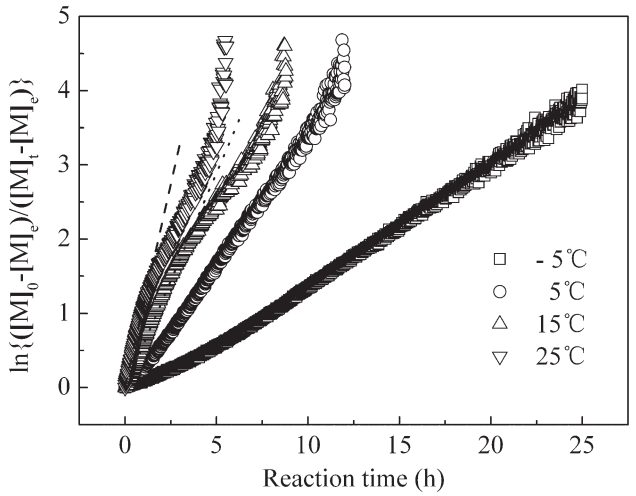

Figure 6. First order plots for the polymerization of THF under different temperatures. Reaction conditions: THF, 20 mL; ECH, 3 mL; HPW, 0.3 g; CH_2Cl_2, 8 mL.

$$M_n + M \underset{k_{dp}}{\overset{k_p}{\rightleftharpoons}} M_{n+1} \quad (1)$$

Where k_p and k_{dp} are the propagation and depolymerization rate constant, respectively.

The molar Gibbs free energy of propagation (ΔG) can be calculated from $[M]_e$ as:

$$\Delta G = RT \ln[M]_e \quad (2)$$

Therefore, the following equations at the equilibrium state can be obtained by Dainton's equation[33] as:

$$\ln[M]_e = \Delta G/RT = (\Delta H_p/RT) - \left(\Delta S_p^0/R\right) \quad (3)$$

Where ΔH_p is the enthalpy change of polymerization under the prevailing experimental conditions, ΔS_p^0 is the entropy change at the standard state ($[M]_e = 1$ mol L^{-1}). Figure 4 shows the

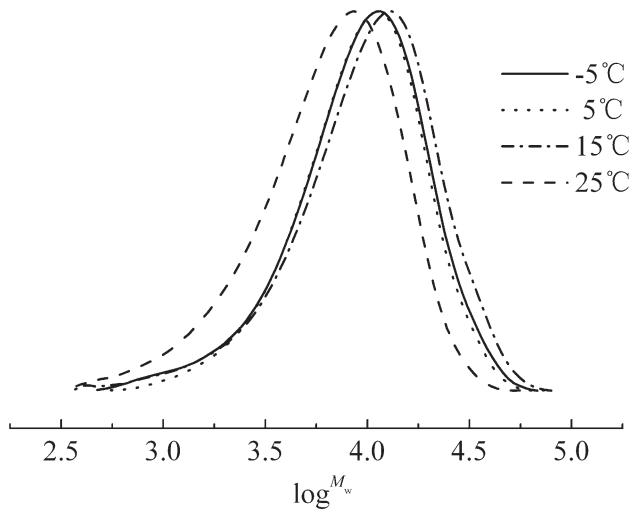

Figure 7. GPC curve evolution of the PTHF samples polymerized at different temperatures. −5°C: $M_w = 11666$, PDI = 1.7; 5°C: $M_w = 11441$, PDI = 1.6; 15°C: $M_w = 12879$, PDI = 1.8; 25°C: $M_w = 8606$, PDI = 1.8.

Table I. The Values of k_{app} at Different Reaction Temperatures[a]

Reaction temperatures (°C)	−5	5	15	25
$k_{app} \times 10^5$ (s^{-1})[b]	4.09[c]	9.51[d]	17.07[e]	31.26[f]

[a] Reaction conditions: THF, 20 mL; ECH, 3 mL; HPW, 0.3 g; CH_2Cl_2, 8 mL.
[b] Determined from the first order plots for the polymerization of THF under different temperatures as eq. (4).
[c] The R-Square of the fitting line for k_{app} is $R^2 = 0.997$.
[d] The R-Square of the fitting line for k_{app} is $R^2 = 0.996$.
[e] The R-Square of the fitting line for k_{app} is $R^2 = 0.999$.
[f] The R-Square of the fitting line for k_{app} is $R^2 = 0.998$.

plots of $\ln[M]_e$ against T^{-1}, which follows eq (3). The thermodynamic parameters calculated from the slope and intercept of the linearly fitted line are: $\Delta H_p = -3.9$ kcal mol^{-1}; $\Delta S_p^0 = -15.3$ cal mol^{-1} K^{-1}). These parameters are both negative as expected, since the heterocyclic monomer polymerization reaction is exothermic due to the release of the five-member ring strain,[31] and they are in excellent accord with the reported values.[10,31] Furthermore, the $[M]_e$ values at 0, 20, and 25°C are calculated to be 1.67, 2.74, and 3.06 mol L^{-1} from eq (3), respectively. They are in good agreement with reported values of $[M]_e$: 1.7 mol L^{-1} (0°C),[34] 2.96 mol L^{-1} (20°C),[34] and 3.1 mol L^{-1} (25°C).[35] Thus, the ceiling temperature T_c at the standard state ($[M] = 1$ mol L^{-1}) can be determined as $T_c = \Delta H_p/\Delta S_p^0 = 255$ K.

Kinetic Investigations

The first-order kinetics of propagation for an equilibrium polymerization of THF is generally expressed as follows,

$$\ln\left\{([M]_0-[M]_e)/([M]_t-[M]_e)\right\} = k_p \times [P^*] \times t = k_{app} \times t \quad (4)$$

Where $[M]_t$ is the monomer concentration at time t, k_p is the apparent second-order rate constant for propagation on the active species, $[P^*]$ is the total concentration of instantaneous propagation species containing the free oxonium ion and ion-pair, which equally contribute to the polymerization of THF.[31] k_{app} is a pseudo first-order rate constant. Such kinetic analysis shows that the propagation rate of THF polymerization is indeed closely related to the propagation species $[P^*]$. The values of $[M]_e$ and $[M]_t$ were both determined from the time dependent spectra monitored by ReactIR.

HPW Concentration. We performed the THF polymerization monitored by *in situ* FTIR under various concentrations of HPW to further understand the effect of HPW concentration on the active propagation species concentration. The plots of $\ln\{([M]_0-[M]_e)/([M]_t-[M]_e)\}$ vs reaction time give a slope equal to the rate constant k_{app} ($k_{app} = k_p \times [P^*]$) for propagation under various concentrations of HPW from 1.2×10^{-3} to 3.6×10^{-3} mol L^{-1} (Figure 5). It could be concluded from the linearity of the plots (Figure 5(a,b,c)) that, at a given HPW concentration, the concentrations of propagation species $[P^*]$ remained approximately constant and the propagation is first-order in monomer at 5°C. The rate constants (k_{app}) for propagation under different HPW concentrations (Figure 5(a,b,c)) were determined to be 2.4×10^{-5}, 5.3×10^{-5}, 8.9×10^{-5} s^{-1}, respectively. Because higher HPW concentration will result in higher active propagation species concentration $[P^*]$ in the equilibrium initiation as Scheme 1(i), it could be observed (Figure 5(a,b,c)) that the increase of rate constants k_{app} is greater than the increase of HPW concentration considering k_p as a constant at a given polymerization temperature. Thus, the assumption that the active species concentration is triple the concentration of HPW in previous literatures[18–21] seems invalid. Besides, as shown in Figure 5d, when the concentration ratio of ECH to HPW ([ECH]/[HPW]) was comparatively low, no further increase of propagation rate could be observed with higher HPW concentration at the early stage of polymerization. This result may indicate that the initiator HPW and promoter ECH have synergistic effect on THF polymerization. Hence, it could be observed that an induction period during initiation step was needed due to low [ECH]/[HPW] ratio, as shown in Figure 5d.

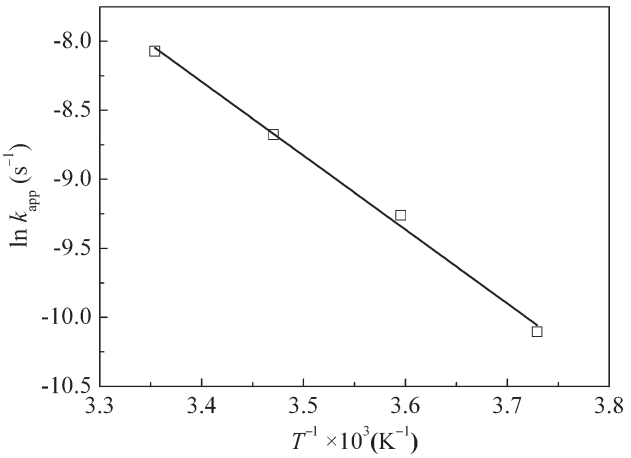

Figure 8. Arrhenius plot for the ring-opening polymerization of THF in CH_2Cl_2 with the linear equation: $\ln k_{app} = -(44530 \times R^{-1}T^{-1}) + \ln 20310$, $R^2 = 0.994$

Polymerization Temperature. Figure 6 shows the plots of $\ln\{([M]_0-[M]_e)/([M]_t-[M]_e)\}$ vs reaction time for THF polymerizations under different temperatures. It is clearly seen from Figure 6 that the plots of $\ln\{([M]_0-[M]_e)/([M]_t-[M]_e)\}$ vs reaction time at −5 and 5°C are linear, which is consistent with a first-order kinetic model, and similar to the results in the bulk[6,17,19–21] and in solvents at low temperature.[36] Besides, our *in situ* kinetic investigations conducted in CH_2Cl_2 at 15 and

Table II. The Values of E_a for THF Polymerization Using Other Initiator Systems

Initiator system	$(CH_3CO)^+ClO_4^-$ [14]	$C_6H_3Cl_2N_2 \cdot PF_6$ [37]	$HClO_4$/Ac [38]	$Al(C_2H_5)_3/H_2O$-ECH [39]
E_a (kJ mol^{-1})	54.5	51.0	50.2	50.2

25°C revealed that the THF polymerization reaction was still found to be first-order at earlier stage of polymerization. However, a noticeable deviation from first-order reaction appeared at later stage of polymerization (Figure 6). A possible explanation for this behavior is the much more occurrence of certain chain-transfer events at the later stage of polymerization, e.g., from polymer to monomer, especially at higher reaction temperatures. This would result in a reduction in the concentration of propagation species. As evident in Figure 7, much more chain transfer events would result in decrease of molecular weight and increase of PDI at 25°C. On the other hand, the concentration of propagation species might not be simply equal to triple the HPW concentration due to the reduction of propagation species in chain transfer reaction, especially at higher reaction temperatures.

Table I lists the k_{app} values of polymerization at different reaction temperatures, which were determined from the slopes of the linear first-order plots as shown in Figure 6. It should be noted that the k_{app} values at 15 and 25°C were determined from the initial slopes of the pseudo first-order plots. Unfortunately, the propagation species concentration $[P^*]$ included in k_{app} could not be determined in our studies due to the complexity of aforementioned chemical equilibrium. Consequently, only the temperature dependence of k_{app} ($k_{app} = k_p \times [P^*]$) was obtained in our studies. The Arrhenius plot of k_{app} vs T^{-1} was linear in the observed temperature range (Figure 8). The apparent activation energy $E_a = 44.53$ kJ mol^{-1} and frequency $A = 2.031 \times 10^4$ are obtained. However, this value of E_a is lower than some literature values that have been reported for THF polymerization using different initiation systems, as listed in Table II.[14,37–39] This may be due to the reasons such as the negative temperature-dependence of ionization oftentimes observed in cationic polymerization because E_a involves both the activation energy for k_p and the temperature dependence of $[P^*]$ at constant [HPW], larger counterion in HPW and different solvent polarity. Because the kinetic studies[14,39] were also carried out in CH_2Cl_2 solvent, the solvent effect could be ignored.

CONCLUSIONS

In this article, we have demonstrated that the *in situ* mid-infrared spectroscopy system (ReactIR) provides a very efficient and reliable spectroscopy technique for a rapid *in situ* tracking of the ring monomer and the linear polymer in the THF polymerization process. Two characteristic infrared peaks at about 1109 and 1068 cm^{-1} can be utilized to easily determine the instantaneous concentrations of the polymer PTHF and monomer THF in reaction mixture by the on-line monitoring system. The *in situ* kinetic investigations indicate that the initiation step using HPW as initiator is an equilibrium reaction. The THF polymerization reaction in CH_2Cl_2 are further confirmed to be typically first order at lower temperatures (−5 and 5°C), and are also found to be first order at earlier stage of polymerization at higher temperatures (15 and 25°C). A deviation from first-order reaction is observed at later stage of polymerization and is raised from much more chain transfer events at higher temperatures.

ACKNOWLEDGMENTS

The authors are grateful to State Key Laboratory of Chemical Engineering at Zhejiang University (Grant No. SKL/ChE-09Z02) for financial supports.

REFERENCES

1. Basko, M.; Bednarek, M.; Billiet, L.; Kubisa, P.; Goethals, E.; Du Prez, F. *J. Polym. Sci. Part A: Polym. Chem.* **2011**, *49*, 1597.
2. Sugi, R.; Tate, D.; Yokozawa, T. *J. Polym. Sci. Part A: Polym. Chem.* **2013**, *51*, 2725.
3. Mah, S.; Hwang, H.; Shin, J. H. *J. Appl. Polym. Sci.* **1999**, *74*, 2637.
4. Chen, Y.; Zhang, G. L.; Zhang, H. Z. *Macromol. Chem. Phys.* **2001**, *202*, 1440.
5. Tasdelen, M. A.; Van Camp, W.; Goethals, E.; Dubois, P.; Du Prez, F.; Yagci, Y. *Macromolecules* **2008**, *41*, 6035.
6. Zhang, A. F.; Zhang, G. L.; Zhang, H. Z. *Macromol. Chem. Phys.* **1999**, *200*, 1846.
7. Szwarc, M. *Macromolecules* **1978**, *11*, 1053.
8. Penczek, S.; Cypryk, M.; Duda, A.; Kubisa, P.; Slomlowski, S. *Prog. Polym. Sci.* **2007**, *32*, 247.
9. Meerwein, V. H.; Hinz, Q.; Hofmann, P. *J. Prakt. Chem.* **1937**, *147*, 257.
10. Buyle, A. M.; Matyjaszewski, K.; Penczek, S. *Macromolecules* **1977**, *10*, 269.
11. Hrkach, J. S.; Matyjaszewski, K. *Macromolecules* **1990**, *23*, 4042.
12. Matyjaszewski, K.; Buyle, A. M.; Penczek, S. *J. Polym. Sci. Polym. Lett. Ed.* **1976**, *14*, 125.
13. Pruckmayr, G.; Wu, T. K. *Macromolecules* **1978**, *11*, 662.
14. Alamo, R.; Guzmán, J.; Fatou, J. G. *Makromol. Chem.* **1981**, *182*, 725.
15. Choi, J.; Kwon, S.; Mah, S. *J. Appl. Polym. Sci.* **2002**, *83*, 2082.
16. Yildiz, S.; Hepuzer, Y.; Yagic, Y.; Pekcan, Ö. *J. Appl. Polym. Sci.* **2003**, *87*, 632.
17. You, L. X.; Hogen-Esch, T. E.; Zhu, Y. H.; Ling, J.; Shen, Z. Q. *Polymer* **2012**, *53*, 4112.
18. Bednarek, M.; Brzezinska, K.; Stasinski, J.; Kubisa, P.; Penczek, S. *Makromol. Chem.* **1989**, *190*, 929.
19. Chen, Y.; Zhang, G. L.; Zhang, H. Z. *J. Appl. Polym. Sci.* **2000**, *77*, 3239.
20. Zhang, A. F.; Zhang, G. L.; Zhang, H. Z. *J. Appl. Polym. Sci.* **1999**, *74*, 1821.
21. Zhang, A. F.; Zhang, G. L.; Zhang, H. Z. *J. Appl. Polym. Sci.* **1999**, *73*, 2303.
22. Bednarek, M.; Kubisa, P.; Penczek, S. *Macromolecules* **1999**, *32*, 5257.
23. Vofsi, D.; Tobolsky, A. *J. Polym. Sci. Part A: Polym. Chem.* **1965**, *3*, 3261.
24. Rodrigues, M. R.; Neumann, M. G. *Macromol. Chem. Phys.* **2001**, *202*, 2776.

25. Storey, R. F.; Maggio, T. L. *Macromolecules* **2000**, *33*, 681.
26. Messman, J. M.; Storey, R. F. *J. Polym. Sci. Part A: Polym. Chem.* **2004**, *42*, 6238.
27. Storey, R. F.; Donnalley, A. B.; Maggio, T. L. *Macromolecules* **1998**, *31*, 1523.
28. Darensbourg, D. J.; Moncada, A. I.; Choi, W.; Reibenspies, J. H. *J. Am. Chem. Soc.* **2008**, *130*, 6523.
29. Weng, S. F. Fourier Transform Infrared Spectrometry Analysis, 2nd ed.; Du, J. X., Xiang, D., Eds.; Chemical Industry Press: Beijing, **2012**; Chapter *8*, pp 317−319.
30. Vivas, M. G.; Mendonca, C. R. *J. Phys. Chem. A* **2012**, *116*, 7033.
31. Penczek, S.; Kubisa, P.; Matjaszewski, K. *Adv. Polym. Sci.* **1985**, *68*, 1.
32. Raquez, J. M.; Degée, P.; Narayan, R.; Dubois, P. *Macromolecules* **2001**, *34*, 8419.
33. Dainton, F. S.; Ivin, K. J. Q. *Rev. Chem. Soc* **1958**, *12*, 61.
34. Ofstead, E. A. *Polym. Prepr. (Am. Chem. Soc. Div. Polym. Chem.)* **1965**, *6*, 674.
35. Afshar-Taromi, F.; Scheer, M.; Rempp, P.; Franta, E. *Makromol. Chem.* **1978**, *179*, 849.
36. Penczek, S. *Macromolecules* **1979**, *12*, 1010.
37. Croucher, T. G.; Wetton, R. E. *Polymer* **1976**, *17*, 205.
38. Guzmán, J.; Sanchez, M. A.; Fatou, G. *An. Quim.* **1978**, *74*, 9.
39. Saegusa, T.; Imai, H.; Matsumoto, S. I. *J. Polym. Sci. Part A-1* **1968**, *6*, 459.